Journal of Organometallic Chemistry, 413 (1991) 321–336
Elsevier Sequoia S.A., Lausanne
JOM 21701

Tetranuclear rhodium–triruthenium carbonyl clusters containing phosphorus(III) ligands; crystal and molecular structure of $[RhRu_3(\mu\text{-}H)_2(\mu\text{-}CO)(CO)_7(PPh_3)_2(\eta^5\text{-}C_5H_5)]$ *

Jean-Luc Le Grand, W. Edward Lindsell * and Kevin J. McCullough *
Chemistry Department, Heriot-Watt University, Riccarton, Edinburgh EH14 4AS (UK)

(Received December 17th, 1990)

Abstract

The reactions of $[RhRu_3(\mu\text{-}H)_2(\mu\text{-}CO)(CO)_9(\eta^5\text{-}C_5H_5)]$ with triphenylphosphine and trimethylphosphite and of $[RhRu_3(\mu\text{-}H)_2(\mu\text{-}CO)(CO)_9(\eta^5\text{-}C_5Me_5)]$ with triphenylphosphine yield clusters $[RhRu_3(\mu\text{-}H)_2(\mu\text{-}CO)(CO)_{9-n}(PR_3)_nCp']$ ($n = 1, 2$; R = Ph, $Cp' = \eta^5\text{-}C_5H_5$, $\eta^5\text{-}C_5Me_5$ and R = OMe, $Cp' = \eta^5\text{-}C_5H_5$) and cleavage products. The structures and isomerisation of the phosphorus containing clusters have been investigated by ^1H and ^{31}P NMR spectroscopy. The crystal structure of $[RhRu_3(\mu\text{-}H)_2(\mu\text{-}CO)(CO)_7(PPh_3)_2(\eta^5\text{-}C_5H_5)]$ has been determined by X-ray diffraction, and the molecule is shown to contain PPh_3 ligands bonded axially and equatorially to two basal ruthenium atoms.

Introduction

Heteronuclear cluster compounds are of interest both in fundamental investigations of the influence of adjacent, different metal centres on the structure and reactivity of organometallics [1] and for their applications as catalysts, or catalyst precursors, for organic reactions [2]. We have previously reported tetranuclear, organometallic clusters containing the catalytically active metals ruthenium and rhodium [3,4]. The asymmetric $RhRu_3$ clusters exhibit geometrical non-rigidity, involving ligand mobility with respect to the metal core [5]; also, facile cleavage of the core occurs on reaction with carbon monoxide [3] and similar cleavage under mild conditions has been noted to be the major result of reaction of $[RhRu_3(\mu\text{-}H)_2(\mu\text{-}CO)(CO)_9(Cp)]$ $\{Cp = (\eta^5\text{-}C_5H_5)\}$ (**1**) with the bidentate phosphorus(III) ligand, 1,2-bis(diphenylphosphino)ethane [5]. However, reaction of cluster **1** with monodentate triphenylphosphine has been shown to produce substituted products $[RhRu_3(\mu\text{-}H)_2(\mu\text{-}CO)(CO)_{9-n}(PPh_3)_n(Cp)]$ $\{n = 1,$ **2**; $n = 2,$ **3**$\}$, although some

---

* Dedicated to Professor Peter L. Pauson on the occasion of his retirement from the Freeland Chair of Chemistry, University of Strathclyde.

accompanying cleavage of the cluster could not be avoided, and NMR studies of **3** support a more stereochemically rigid system for this phosphine-containing cluster [5].

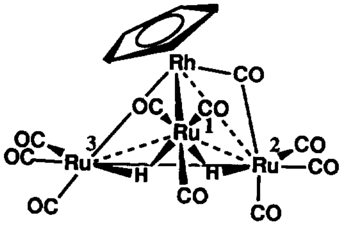

1

In this paper, the reaction of **1** with triphenylphosphine has been further characterised, in particular through a structural investigation by X-ray analysis of the crystalline product $[RhRu_3(\mu\text{-}H)_2(\mu\text{-}CO)(CO)_7(PPh_3)_2Cp]$ (**3**). Also presented are related reactions of trimethylphosphite with **1** and of triphenylphosphine with $[RhRu_3(\mu\text{-}H)_2(\mu\text{-}CO)(CO)_9(Cp^\star)]$ $\{Cp^\star = (\eta^5\text{-}C_5Me_5)\}$ (**4**), from which phosphorus(III)-containing $RhRu_3$ clusters are obtained.

Results and discussion

Reaction of $[RhRu_3(\mu\text{-}H)_2(\mu\text{-}CO)(CO)_9Cp]$ (1) with triphenylphosphine

Reactions of $[RhRu_3(\mu\text{-}H)_2(\mu\text{-}CO)(CO)_9(Cp)]$ (**1**) with triphenylphosphine in molar ratios 1 : 1–2, at ambient temperature, produce a mixture of mono- and di-substituted clusters $[RhRu_3(\mu\text{-}H)_2(\mu\text{-}CO)(CO)_{9-n}(PPh_3)_nCp]$ ($n = 1$, **2**; $n = 2$, **3**) [5] and cleavage products, separable by chromatography, but no detectable tri-substituted, tetranuclear $RhRu_3$ clusters. The only identified Rh-containing cleavage product has been $[Rh(CO)_2Cp]$; elution with dichloromethane/acetone from a silica gel column separates several distinct yellow bands which, from spectroscopic studies, appear to comprise at least two ruthenium species, containing CO and aromatic phosphine ligands, and without RhCp units. These non-crystalline products are not simple clusters, $[Ru_3(CO)_{12-n}(PPh_3)_n]$, and may be products resulting from oxidative addition reactions of PPh_3 to a cleaved Ru_n fragment but, in the absence of a crystallographic study, their structures cannot be assigned.

Previous ^1H, ^{13}C and ^{31}P NMR studies on cluster **2** in solution [5] have established the existence of two main isomeric forms which undergo rapid interchange at room temperature. The principal isomer (ca. 83%) with structure **2a** is more fluxional; the other form probably has structure **2b**, see below, and is rigid on the ^1H NMR time-scale at $-90\,^\circ C$ [5]. The fact that **2a** is highly fluxional can be rationalised in terms of the lowest energy rearrangement process which involves concerted reorientation of the CO ligands around the RhRu(2)Ru(3) face so that bridging by a CO ligand oscillates between the Rh–Ru(2) and Rh–Ru(3) bonds causing enantiomerisation **i** $\rightleftharpoons$ **ii**. A similar interconversion for **2b** would create a third isomer **2c** which, although it may be present in low concentration, cannot be detected by NMR spectroscopy and is probably thermodynamically unfavorable; also, a simple interconversion of CO ligands around the RhRu(2)Ru(3) face is prevented by the presence of the PPh_3 group at Ru(2).

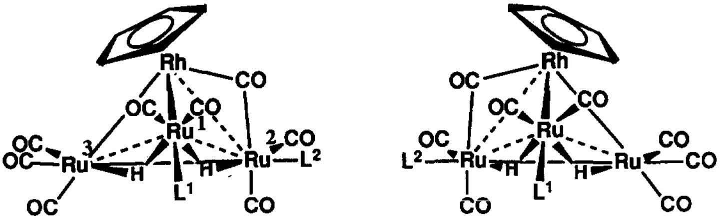

(i) (ii)

2a L^1 = PPh_3, L^2 = CO (major isomer)
2b L^1 = CO, L^2 = PPh_3 (minor isomer)
3 L^1 = L^2 = PPh_3
5 L^1 = $P(OMe)_3$, L^2 = CO (major isomer)
6 L^1 = L^2 = $P(OMe)_3$

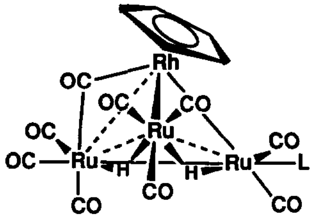

2c L = PPh_3
(possible third isomer)

Cluster 3 is rigid on the NMR time-scale at room temperature and a probable structure with PPh_3 ligands coordinated to atoms Ru(1) and Ru(2), as in representation 3, can be deduced from ^1H, ^{13}C and ^{31}P NMR spectra [5] (e.g. see Table 1). The coordination sites appear to be those occupied by single PPh_3 ligands in the isomers **2a** and **2b** of cluster **2**. However, the alternative coordination of PPh_3 groups to Ru(1) and Ru(3) cannot be definitively ruled out and the relative orientation of the PPh_3 ligands with respect to the $RhRu_3$ framework, i.e. axial or equatorial, and to the other ligands, CO and H, is not clear from these spectral studies. In fact the value of J(Rh–P) for $L^2 = PPh_3$ (18.1 Hz) is large in comparison to that of L^1 (3.7 Hz), whereas L^1 is predicted to be *cis* to the hydride ligands (from J(H–P) values), and hence *trans* to the Rh–Ru(1) bond in an axial site. This could imply that L^2 was also axial and *trans* to Rh to account for the large values of J(Rh–P). To resolve these uncertainties, to gain a clearer insight into the substitution pathways of the parent cluster **1** and to monitor the structural effects of the phosphine ligands on the tetranuclear system, the crystal structure of **3** was determined.

Structural studies on [$RhRu_3(\mu\text{-}H)_2(\mu\text{-}CO)(CO)_7(PPh_3)_2Cp$] (3)

A dark red-brown thin plate of **3**, obtained from dichloromethane/hexane at −15 °C, was subjected to analysis by X-ray diffraction. The resultant molecular structure of one asymmetric unit is depicted in Fig. 1, and Tables 2 and 3 list, respectively, atomic fractional coordinates and the more important geometrical parameters. The structure is closely related to that of the parent **1** [3], with an

Table 1

Selected NMR resonances of triruthenium–rhodium clusters at 25 °C

Complex	^{1}H NMR δ ppm (coupling) (hydride resonances)	Solvent	^{31}P{^{1}H} NMR δ ppm (coupling)	Solvent	Comments	Ref.
$[RhRu_3(\mu\text{-H})_2(\mu\text{-CO})(CO)_9Cp]$	−17.23 (s, 2H)	$CDCl_3$;			fluxional, fast exchange	5
$[RhRu_3(\mu\text{-H})_2(\mu\text{-CO})(CO)_8(PPh_3)Cp]$	−16.21 (d, *J*(P–H) 8 Hz; 2H)	CD_2Cl_2;	39.0 (s, br)	$CDCl_3$	fluxional, rel. fast exchange (two isomers at low temp.)	5
$[RhRu_3(\mu\text{-H})_2(\mu\text{-CO})(CO)_7(PPh_3)_2Cp]$	−15.07 (ddd, *J*(P–H) 13.6 and 2, *J*(H–H) 2 Hz; 1H) −16.48 (ddd, *J*(P–H) 7.0 and 9, *J*(H–H) 2 Hz; 1H)	CD_2Cl_2;	45.25 (d, *J*(Rh–P) 18.1 Hz; P^2) 31.7 (d, *J*(Rh–P) 3.7 Hz; P^1)	$CDCl_3$	rigid	5
$[RhRu_3(\mu\text{-H})_2(\mu\text{-CO})(CO)_8\{P(OMe)_3\}Cp]$	−17.13 (d, br, *J*(P–H) 8.6 Hz, 2H)	CD_2Cl_2;	142.9 (s, br, 1P)	CD_2Cl_2	fluxional	
$[RhRu_3(\mu\text{-H})_2(\mu\text{-CO})(CO)_7\{P(OMe)_3\}_2Cp]$	−16.3 (s, br, 1H) −17.9 (s, br, 1H)	$CDCl_3$;		$CDCl_3$	fluxional, slow exchange at r.t.	
	−16.25 (ddd, *J*(P–H) 10.4 and 2, *J*(H–H) 2.4 Hz; 1H) [a] −18.05 (ddd, *J*(P–H) 9 and 9, *J*(H–H) 2.4 Hz; 1H) [a]	$CDCl_3$;	158.2 (d, *J*(Rh–P) 22.9 Hz, P^2) [a] 144.6 (s, P^1) [a]	$CDCl_3$	rigid at −25 °C	
$[RhRu_3(\mu\text{-H})_2(\mu\text{-CO})(CO)_9Cp^*]$ (i) (ii)	−13.22 (s, 1H) −20.61 (s, 1H) −17.24 (d, *J*(Rh–H) 8.7 Hz, 2H)	CD_2Cl_2;			isomer **4b**, 20%, rigid isomer(s), **4a** mainly, 80%, fast exchange	5
$[RhRu_3(\mu\text{-H})_2(\mu\text{-CO})(CO)_8(PPh_3)Cp^*]$	−13.01 (d, *J*(P–H) 9.9 Hz, 1H) −20.62 (d, *J*(P–H) 2.8 Hz, 1H)	CD_2Cl_2;	34.1 (s)	CD_2Cl_2	slow exchange (no change at low temp.)	
$[RhRu_3(\mu\text{-H})_2(\mu\text{-CO})(CO)_7(PPh_3)_2Cp^*]$	−12.28 (ddd, *J*(P–H) 13.2 and 7.8, *J* <1 Hz, 1H) −20.34 (dd, *J*(P–H) 10.2 and 2.8 Hz, 1H)	$CDCl_3$;	41.6 (d, *J*(Rh–P) 3.1 Hz, 1P) 29.9 (s, 1P)	$CDCl_3$	rigid	

[a] At −25 °C.

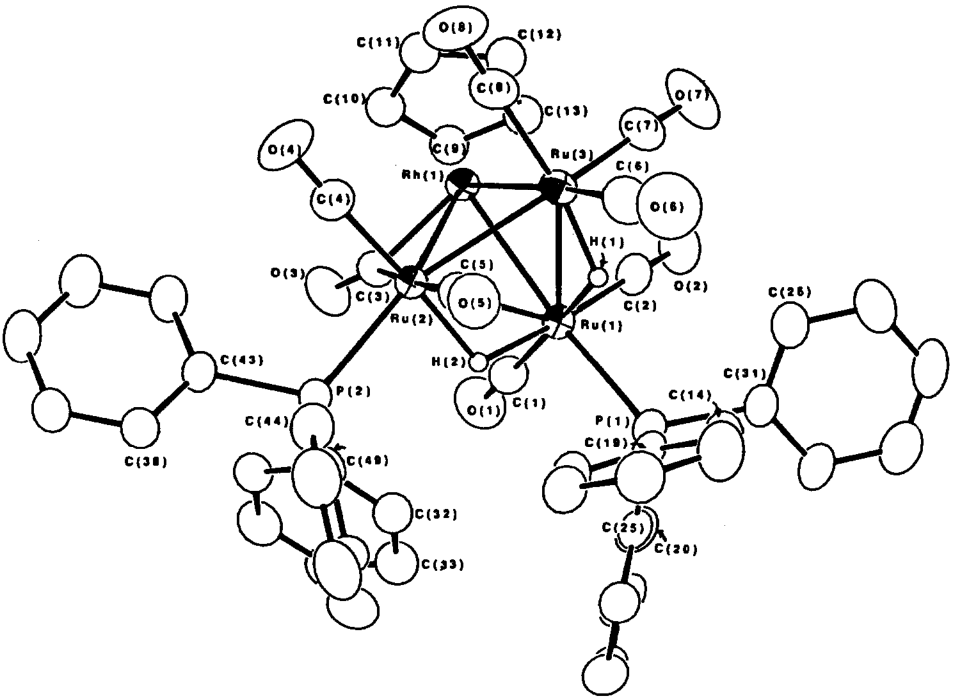

Fig. 1. The molecular structure of cluster **3** (ORTEP [11], 50% probability ellipsoids). Labels for the atoms of the phenyl rings have been omitted for clarity.

approximately tetrahedral arrangement of metal atoms, a cyclopentadienyl ligand η^5-coordinated to Rh, two μ-H atoms spanning Ru(1)–Ru(2) and Ru(1)–Ru(3), a μ-CO group bridging Rh–Ru(2) and the remaining seven CO ligands terminally bonded to the Ru atoms. The phosphine ligands are bonded to atoms Ru(1) and Ru(2) and, as in **1**, the distribution of ligands (CO, H and PPh_3) and adjacent bonded, non-bridged metal atom(s) (Rh and Ru) around each Ru atom is roughly octahedral, as illustrated in Fig. 2.

Ligands $P(1)Ph_3$ and $P(2)Ph_3$ are located at Ru(1) and Ru(2), respectively, as suggested by NMR and IR spectra. P(1) is in an axial site and *trans* to the Rh–Ru(1) bond (angle Rh–Ru(1)–P(1) = 166.39(3)°), whereas P(2) is essentially in an equatorial site, *trans* to Ru(3) (angle Ru(3)–Ru(2)–P(2) = 160.79(3)°) and close to the Ru_3 plane: comparable angles for the corresponding *trans* CO ligands in **1** are 173.7(2)° and 166.6(2)°, respectively. Related metal–metal distances in clusters **1** and **3** lie within ±0.03 Å, with the largest divergence occurring for the carbonyl-bridged bond Rh–Ru(2) (2.727(1) Å in **1**; 2.6964(5) Å in **3**). The terminal CO groups in clusters **1** and **3** are in geometrically related sites but there is a significant difference in the positions, and presumably the bonding, of the bridging CO ligands. In **1** the bridging CO is asymmetric, interacting more with Rh (Rh–C = 1.924(5) Å; Ru(2)–C = 2.220(5) Å), whereas in **3** a more symmetrical arrangement occurs (Rh–C = 1.991(5) Å; Ru(2)–C = 2.095(5) Å). This difference must be primarily due to the influence of the *cis*-$P(2)Ph_3$ ligand and is reflected in the decrease in frequency of the IR active $\nu(\mu$-CO) band on substitution (1827 cm^{-1} (**1**); 1780

Table 2

Fractional coordinates of atoms with standard deviations

	x	y	z	U_e
Rh(1)	0.38262(3)	0.91980(3)	0.84609(2)	0.0292(2)
Ru(1)	0.31199(3)	0.96966(3)	0.72110(2)	0.0267(2)
Ru(2)	0.19879(3)	1.04503(3)	0.85052(2)	0.0257(2)
Ru(3)	0.13733(3)	0.80393(3)	0.81448(2)	0.0323(2)
P(1)	0.20206(11)	0.98384(11)	0.62320(6)	0.0318(6)
P(2)	0.20488(10)	1.25186(10)	0.85154(6)	0.0284(6)
C(1)	0.4648(5)	1.0968(4)	0.70419(24)	0.039(3)
O(1)	0.5601(4)	1.1710(3)	0.69420(22)	0.061(3)
C(2)	0.4012(5)	0.8598(4)	0.68385(24)	0.040(3)
O(2)	0.4551(4)	0.7933(4)	0.66013(20)	0.060(3)
C(3)	0.4045(4)	1.0959(4)	0.85515(23)	0.034(3)
O(3)	0.4930(3)	1.1794(3)	0.86382(21)	0.0514(23)
C(4)	0.1691(5)	1.0237(5)	0.9448(3)	0.043(3)
O(4)	0.1528(4)	1.0057(4)	1.00177(19)	0.071(3)
C(5)	0.0122(4)	0.9841(4)	0.84021(23)	0.036(3)
O(5)	−0.0998(3)	0.9628(3)	0.84058(20)	0.0551(25)
C(6)	−0.0396(5)	0.7361(5)	0.7902(3)	0.053(4)
O(6)	−0.1433(4)	0.6933(5)	0.7755(3)	0.089(4)
C(7)	0.2018(5)	0.6741(5)	0.7825(3)	0.050(3)
O(7)	0.2446(5)	0.6003(4)	0.7599(3)	0.079(3)
C(8)	0.1075(5)	0.7570(5)	0.9075(3)	0.050(3)
O(8)	0.0917(5)	0.7283(4)	0.96296(23)	0.081(3)
C(9)	0.5917(4)	0.9170(4)	0.85120(21)	0.0439(0)
C(10)	0.5418(4)	0.9305(4)	0.91884(21)	0.0439(0)
C(11)	0.4386(4)	0.8262(4)	0.93612(21)	0.0439(0)
C(12)	0.4246(4)	0.7483(4)	0.87917(21)	0.0439(0)
C(13)	0.5192(4)	0.8044(4)	0.82668(21)	0.0439(0)
C(9′)	0.5707(14)	0.9381(10)	0.8992(7)	0.0280(0)
C(10′)	0.4666(14)	0.8626(10)	0.9406(7)	0.0280(0)
C(11′)	0.4119(14)	0.7580(10)	0.9027(7)	0.0280(0)
C(12′)	0.4821(14)	0.7688(10)	0.8379(7)	0.0280(0)
C(13′)	0.5803(14)	0.8801(10)	0.8357(7)	0.0280(0)
C(14)	−0.0733(3)	0.8885(3)	0.61661(17)	0.050(3)
C(15)	−0.2051(3)	0.8852(3)	0.63437(17)	0.057(4)
C(16)	−0.2358(3)	0.9747(3)	0.67567(17)	0.053(3)
C(17)	−0.1349(3)	1.0673(3)	0.69922(17)	0.045(3)
C(18)	−0.0032(3)	1.0706(3)	0.68147(17)	0.043(3)
C(19)	0.0276(3)	0.9812(3)	0.64016(17)	0.0322(24)
C(20)	0.4040(3)	1.1366(3)	0.54547(17)	0.053(3)
C(21)	0.4645(3)	1.2382(3)	0.50615(17)	0.067(4)
C(22)	0.3925(3)	1.3186(3)	0.49013(17)	0.073(5)
C(23)	0.2599(3)	1.2974(3)	0.51342(17)	0.069(4)
C(24)	0.1994(3)	1.1959(3)	0.55274(17)	0.052(3)
C(25)	0.2714(3)	1.1155(3)	0.56876(17)	0.039(3)
C(26)	0.1646(4)	0.7416(3)	0.59195(13)	0.047(3)
C(27)	0.1495(4)	0.6421(3)	0.54930(13)	0.065(4)
C(28)	0.1612(4)	0.6578(3)	0.47896(13)	0.071(5)
C(29)	0.1879(4)	0.7728(3)	0.45128(13)	0.072(5)
C(30)	0.2030(4)	0.8723(3)	0.49393(13)	0.056(4)
C(31)	0.1914(4)	0.8567(3)	0.56427(13)	0.037(3)
C(32)	0.3345(3)	1.3314(3)	0.72532(14)	0.045(3)
C(33)	0.4347(3)	1.4020(3)	0.68204(14)	0.058(4)

Table 2 (continued)

	x	y	z	U_e
C(34)	0.5368(3)	1.4894(3)	0.70888(14)	0.057(4)
C(35)	0.5386(3)	1.5062(3)	0.77899(14)	0.049(3)
C(36)	0.4383(3)	1.4356(3)	0.82226(14)	0.040(3)
C(37)	0.3363(3)	1.3482(3)	0.79543(14)	0.0321(24)
C(38)	0.1754(3)	1.4294(3)	0.94626(14)	0.042(3)
C(39)	0.1971(3)	1.4916(3)	1.00728(14)	0.054(3)
C(40)	0.2714(3)	1.4562(3)	1.05491(14)	0.073(5)
C(41)	0.3241(3)	1.3585(3)	1.04150(14)	0.083(5)
C(42)	0.3025(3)	1.2962(3)	0.98048(14)	0.059(4)
C(43)	0.2281(3)	1.3317(3)	0.93285(14)	0.0340(25)
C(44)	−0.0612(3)	1.2340(3)	0.87140(14)	0.044(3)
C(45)	−0.1817(3)	1.2568(3)	0.85975(14)	0.056(4)
C(46)	−0.1906(3)	1.3283(3)	0.80486(14)	0.063(4)
C(47)	−0.0790(3)	1.3771(3)	0.76161(14)	0.065(4)
C(48)	0.0415(3)	1.3542(3)	0.77325(14)	0.043(3)
C(49)	0.0504(3)	1.2827(3)	0.82815(14)	0.0344(25)
H(1)	0.158(6)	0.859(5)	0.738(3)	0.066(18)
H(2)	0.239(5)	1.076(4)	0.7618(24)	0.043(14)

cm^{-1} (**3**); in hexane [5]). In both **3** and **1** the μ-CO group lies close to the Rh–Ru(2)–Ru(3) plane with exterior interplanar angles Rh–C–Ru(2)/Rh–Ru(2)–Ru(3) of 168.9° and 169.5°, respectively. It seems unusual that, in the ^{31}P NMR spectrum of **3**, a low value is observed for the J(Rh–P) coupling constant to the axial atom, P(1), *trans* to Rh, whereas a larger coupling constant occurs to the equatorial atom, P(2), *cis* to the bridging-CO ligand (angle C(3)–Ru(2)–P(2) = 87.97(13)°) and *cisoid* to Rh (angle Rh–Ru(2)–P(2) = 134.85(3)°). The larger coupling must result from the electronic interaction of the bridging Rh–μ-CO–Ru system with the *cis*-phosphine.

The cyclopentadienyl ligand is canted away from the Rh–μ-CO–Ru(2) system with the interior angle between the plane of the C_5-ring and the Ru_3-plane of 20.0° (cf. 22° for the related angle in **1**). The bridging hydrogen ligands lie below the Ru_3-plane and relevant exterior interplanar angles are: Ru(1)–H(1)–Ru(3)/Ru_3 118.6°; Ru(1)–H(2)–Ru(2)/Ru_3 137.4°.

This structural characterisation of **3** supports structures **2a** and **2b** as being the major and minor isomeric forms, respectively, of **2** and, since rapid equilibration between species occurs in solution, this indicates that substitution axially at Ru(1) and, secondly, equatorially at Ru(2) produces the most stable derivatives. A structure related to **3** has been proposed for the di-phosphorus(III) containing clusters $[FeRu_3(\mu\text{-}H)_2(\mu\text{-}CO)_2(CO)_{11-n}(PR_3)_n]$ ($n = 2$), with isomers analogous to **2a** and **2b** for mono-substituted derivatives ($n = 1$) but, although the structure of type **2a** with an axial phosphine ligand was confirmed by X-ray analysis ($PR_3 = PMe_2Ph$; $n = 1$), the orientation of the phosphorus ligand in the other isomer, or of the second phosphorus ligand in $FeRu_3$ clusters with $n = 2$, was not definitively established [6]. It may be noted that only axial substitution of heteronuclear tetrahedral clusters occurs in the formation of phosphorus derivatives $[NiOs_3(\mu\text{-}H)_3(CO)_7(PMe_2Ph)_2Cp]$ [7] and $[FeCo_3(\mu_3\text{-}H)(CO)_9\{P(OMe)_3\}_3]$ [8].

Table 3

Selected derived geometrical parameters for 3

a. Bond lengths (Å) with standard deviations

Rh(1)–Ru(1)	2.7381(5)	Rh(1)–C(11)	2.283(4)
Rh(1)–Ru(2)	2.6964(5)	Rh(1)–C(12)	2.254(4)
Rh(1)–Ru(3)	2.6876(5)	Rh(1)–C(13)	2.212(4)
Rh(1)–C(3)	1.991(5)	Rh(1)–C(9′)	2.263(14)
Ru(1)–Ru(2)	2.9558(5)	Rh(1)–C(10′)	2.296(14)
Ru(1)–Ru(3)	2.8644(5)	Rh(1)–C(11′)	2.291(14)
Ru(1)–P(1)	2.3504(13)	Rh(1)–C(12′)	2.255(14)
Ru(1)–C(1)	1.883(5)	Rh(1)–C(13′)	2.237(14)
Ru(1)–C(2)	1.878(5)	P(1)–C(19)	1.833(3)
Ru(1)–H(1)	1.79(6)	P(1)–C(25)	1.830(4)
Ru(1)–H(2)	1.77(5)	P(1)–C(31)	1.843(4)
Ru(2)–Ru(3)	2.7799(5)	P(2)–C(37)	1.839(3)
Ru(2)–P(2)	2.3708(12)	P(2)–C(43)	1.837(3)
Ru(2)–C(3)	2.095(5)	P(2)–C(49)	1.842(3)
Ru(2)–C(4)	1.873(5)	C(1)–O(1)	1.141(6)
Ru(2)–C(5)	1.927(5)	C(2)–O(2)	1.144(6)
Ru(2)–H(2)	1.79(5)	C(3)–O(3)	1.171(6)
Ru(3)–C(6)	1.912(6)	C(4)–O(4)	1.140(7)
Ru(3)–C(7)	1.883(6)	C(5)–O(5)	1.137(6)
Ru(3)–C(8)	1.902(6)	C(6)–O(6)	1.129(8)
Ru(3)–H(1)	1.63(6)	C(7)–O(7)	1.135(7)
Rh(1)–C(9)	2.216(4)	C(8)–O(8)	1.137(8)
Rh(1)–C(10)	2.261(4)		

b. Angles (°) with standard deviations

Ru(1)–Rh(1)–Ru(2)	65.894(13)	Ru(3)–Ru(2)–C(3)	105.13(13)
Ru(1)–Rh(1)–Ru(3)	63.723(13)	Ru(3)–Ru(2)–C(4)	97.74(16)
Ru(1)–Rh(1)–C(3)	80.04(13)	Ru(3)–Ru(2)–C(5)	69.13(14)
Ru(2)–Rh(1)–Ru(3)	62.171(13)	Ru(3)–Ru(2)–H(2)	86.3(16)
Ru(2)–Rh(1)–C(3)	50.40(13)	P(2)–Ru(2)–C(3)	87.97(13)
Ru(3)–Rh(1)–C(3)	111.79(13)	P(2)–Ru(2)–C(4)	95.54(16)
Rh(1)–Ru(1)–Ru(2)	56.376(12)	P(2)–Ru(2)–C(5)	97.07(14)
Rh(1)–Ru(1)–Ru(3)	57.280(12)	P(2)–Ru(2)–H(2)	81.3(16)
Rh(1)–Ru(1)–P(1)	166.39(3)	C(3)–Ru(2)–C(4)	92.81(20)
Rh(1)–Ru(1)–C(1)	93.43(15)	C(3)–Ru(2)–C(5)	173.84(19)
Rh(1)–Ru(1)–C(2)	88.11(15)	C(3)–Ru(2)–H(2)	83.3(16)
Rh(1)–Ru(1)–H(1)	88.5(19)	C(4)–Ru(2)–C(5)	90.23(21)
Rh(1)–Ru(1)–H(2)	87.5(16)	C(4)–Ru(2)–H(2)	175.1(16)
Ru(2)–Ru(1)–Ru(3)	57.035(12)	C(5)–Ru(2)–H(2)	93.9(16)
Ru(2)–Ru(1)–P(1)	116.77(3)	Rh(1)–Ru(3)–Ru(1)	58.997(13)
Ru(2)–Ru(1)–C(1)	101.69(15)	Rh(1)–Ru(3)–Ru(2)	59.071(13)
Ru(2)–Ru(1)–C(2)	142.69(15)	Rh(1)–Ru(3)–C(6)	174.55(18)
Ru(2)–Ru(1)–H(1)	75.3(19)	Rh(1)–Ru(3)–C(7)	89.23(17)
Ru(2)–Ru(1)–H(2)	34.2(16)	Rh(1)–Ru(3)–C(8)	85.72(17)
Ru(3)–Ru(1)–P(1)	109.18(3)	Rh(1)–Ru(3)–H(1)	93.6(20)
Ru(3)–Ru(1)–C(1)	149.60(15)	Ru(1)–Ru(3)–Ru(2)	63.140(13)
Ru(3)–Ru(1)–C(2)	95.96(15)	Ru(1)–Ru(3)–C(6)	117.69(18)
Ru(3)–Ru(1)–H(1)	31.4(19)	Ru(1)–Ru(3)–C(7)	92.88(17)
Ru(3)–Ru(1)–H(2)	84.0(16)	Ru(1)–Ru(3)–C(8)	143.17(17)
P(1)–Ru(1)–C(1)	99.72(15)	Ru(1)–Ru(3)–H(1)	34.8(20)
P(1)–Ru(1)–C(2)	95.21(15)	Ru(2)–Ru(3)–C(6)	115.84(18)
P(1)–Ru(1)–H(1)	78.1(19)	Ru(2)–Ru(3)–C(7)	146.64(17)
P(1)–Ru(1)–H(2)	89.7(16)	Ru(2)–Ru(3)–C(8)	90.95(17)

Table 3 (continued)

b. Angles (°) with standard deviations

C(1)–Ru(1)–C(2)	90.49(21)	Ru(2)–Ru(3)–H(1)	82.7(20)
C(1)–Ru(1)–H(1)	174.6(19)	C(6)–Ru(3)–C(7)	95.38(25)
C(1)–Ru(1)–H(2)	87.0(16)	C(6)–Ru(3)–C(8)	96.57(25)
C(2)–Ru(1)–H(1)	94.6(19)	C(6)–Ru(3)–H(1)	83.5(21)
C(2)–Ru(1)–H(2)	174.8(16)	C(7)–Ru(3)–C(8)	97.15(24)
H(1)–Ru(1)–H(2)	88.1(24)	C(7)–Ru(3)–H(1)	89.8(21)
Rh(1)–Ru(2)–Ru(1)	57.731(12)	C(8)–Ru(3)–H(1)	173.0(21)
Rh(1)–Ru(2)–Ru(3)	58.758(13)	Ru(1)–C(1)–O(1)	177.6(4)
Rh(1)–Ru(2)–P(2)	134.85(3)	Ru(1)–C(2)–O(2)	178.9(4)
Rh(1)–Ru(2)–C(3)	47.06(12)	Rh(1)–C(3)–Ru(2)	82.53(17)
Rh(1)–Ru(2)–C(4)	91.19(16)	Rh(1)–C(3)–O(3)	135.3(4)
Rh(1)–Ru(2)–C(5)	127.57(14)	Ru(2)–C(3)–O(3)	142.0(4)
Rh(1)–Ru(2)–H(2)	88.4(16)	Ru(2)–C(4)–O(4)	176.7(5)
Ru(1)–Ru(2)–Ru(3)	59.826(12)	Ru(2)–C(5)–O(5)	169.2(4)
Ru(1)–Ru(2)–P(2)	112.66(3)	Ru(3)–C(6)–O(6)	178.1(5)
Ru(1)–Ru(2)–C(3)	73.33(12)	Ru(3)–C(7)–O(7)	175.7(5)
Ru(1)–Ru(2)–C(4)	147.57(16)	Ru(3)–C(8)–O(8)	178.8(5)
Ru(1)–Ru(2)–C(5)	101.35(14)	Ru(1)–H(1)–Ru(3)	113.7(33)
Ru(1)–Ru(2)–H(2)	33.7(16)	Ru(1)–H(2)–Ru(2)	112.1(26)
Ru(3)–Ru(2)–P(2)	160.79(3)		

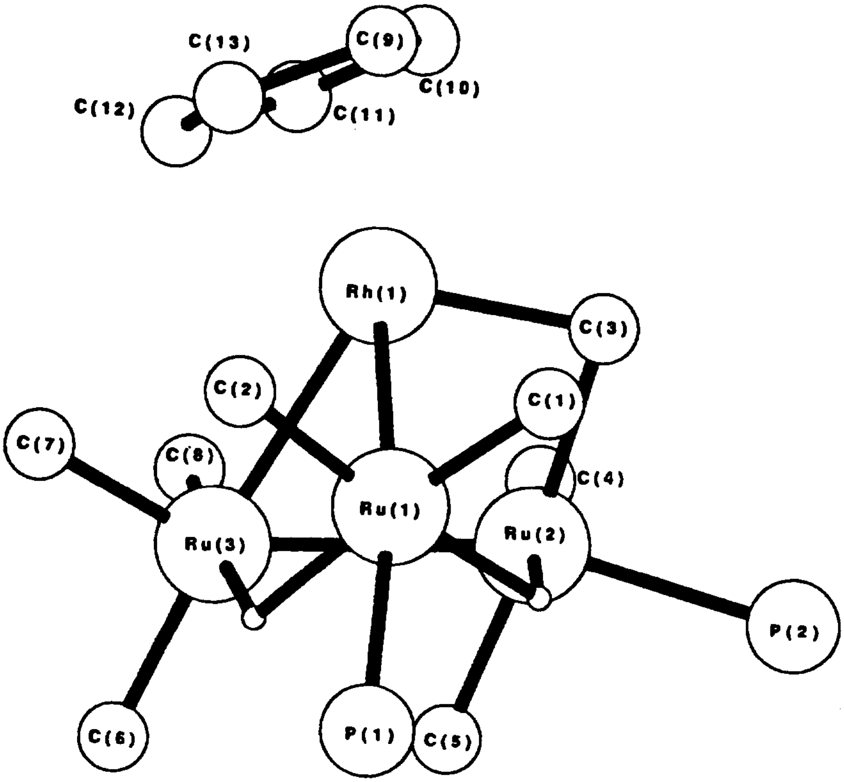

Fig. 2. The molecular structure of 3 (PLUTO [11]) in the region of the $RhRu_3$ cluster.

Complex **3** displays simple NMR spectra at ambient temperature, consistent with the solid state structure. In toluene-d_8 solution, the well-resolved hydride resonances in the ^{1}H NMR spectrum at 19 °C {−14.80 ppm (ddd, 14.2, 2, 2.6 Hz); −16.18 ppm (ddd, 9.3, 7.1, 2.6 Hz)} broaden on heating, with complete loss of resolution by 50 °C. At higher temperatures further broadening occurs but no simple coalescence is observed. Decomposition sets in, producing at 80 °C a species with a doublet hydride resonance and this is the only high-field signal present at 110 °C (−16.11 ppm, d, 9.2 Hz). On subsequent cooling of this heated solution to 19 °C the resonance changes into a broad band (−16.1 ppm, half-width > 20 Hz). Two new metal carbonyl species were separated by chromatography of this thermally decomposed system, and of related reactions conducted in non-deuteriated toluene, but these products were not conclusively identified. Thus, cluster **3** initially appears to become geometrically non-rigid on the ^{1}H NMR time-scale at elevated temperatures but then around 90–100 °C undergoes complete thermal decomposition.

Reaction of $[RhRu_3(\mu\text{-}H)_2(\mu\text{-}CO)(CO)_9Cp]$ *(1) with trimethylphosphite*

The reaction of **1** with $P(OMe)_3$ in THF at ambient temperature affords, after chromatography, two substituted clusters $[RhRu_3(\mu\text{-}H)_2(\mu\text{-}CO)(CO)_{9-n}\{P(OMe)_3)_nCp]$ ($n = 1$, **5**; $n = 2$, **6**)), as well as $[Rh(CO)_2Cp]$ and other uncharacterised clusters. Reactions carried out in the presence of Me_3NO give similar results. Compounds **5** and **6** are obtained in relatively low yields but appear from spectroscopic studies to be structurally related to **2** and **3**, respectively, and this indicates that substitution reactions of **1** by the mono-phosphorus ligands take similar pathways.

Cluster **5** could only be obtained as a slightly oily solid so that a sample free of residual hydrocarbon could not be obtained for elemental analysis but the FAB mass spectrum included a well-defined parent ion and ions arising from the consecutive loss of nine CO groups. It should be noted that small ion peaks with *m/e* values corresponding to species with 1, 2 and 3 more CO groups than in the parent were also evident and these could arise from redistribution reactions during analysis (cf. reported cluster redistribution occuring on mass spectral investigation of $[Co_3Rh(CO)_9\{P(OMe)_3\}_3]$ [9]) or may be due to minor impurities which could account for the oily nature of the product. The ^{1}H and $^{31}P\{^1H\}$ NMR spectra of **5** at 25 °C (see Table 1 and Experimental Section) are comparable to those of **2** with a broadened ^{1}H metal–hydrogen doublet resonance (J(P–H) 8.6 Hz, half-width ca. 5 Hz) and a broad ^{31}P resonance (half-width ca. 200 Hz) indicating the occurrence of some exchange process; a prominent band assignable to a $\nu(\mu\text{-}CO)$ vibration occurs in the IR spectrum at 1823 cm^{-1}, consistent with an isomer of structure **2a**, but a very weak band at 1789 cm^{-1} could be due to an isomer of the type **2b**. Thus, **5** probably exhibits isomerisation and fluxionality similar to cluster **2**.

$[RhRu_3(\mu\text{-}H)_2(\mu\text{-}CO)(CO)_7\{P(OMe)_3\}_2Cp]$ (**6**) can be obtained as analytically pure crystals. The NMR spectra at 25 °C are broadened so that some exchange occurs under these conditions but, at −25 °C well-resolved ^{1}H and $^{31}P\{^1H\}$ spectra are assignable to a single rigid species of structure related to that of **3** (see Table 1 and Experimental Section). The J(P–H) constants were assigned by selective ^{31}P decoupling experiments; a coupling of ^{103}Rh to P^2 (22.9 Hz) in the $^{31}P\{^1H\}$ NMR spectrum was observed, but the expected smaller Rh–P coupling to P^1 could not be resolved (half-width of resonance = ca. 9 Hz). Structure **3** is also consistent with the lower $\nu(\mu\text{-CO})$ band in the IR spectrum (1782 cm^{-1}).

Reaction of $[RhRu_3(\mu\text{-}H)_2(\mu\text{-}CO)(CO)_9Cp^\star]$ *(4) with triphenylphosphine*

In the solid state cluster **4** adopts structure **4a** with the hydrogen ligands bridging one Ru–Ru and one Rh–Ru bond, as determined by X-ray crystallography [3]. However, in solution isomerisation occurs and a second isomer is present (ca. 20%) which appears to be rigid on the ^1H NMR time-scale. This isomer can be assigned structure **4b** [5], analogous to the single, fluxional form of cluster **1**. The main isomeric form in solution is **4a** but this is fluxional even at relatively low temperatures in ^1H and ^{13}C NMR spectra and is in dynamic equilibrium with a third form, present in low concentration [5]. Hence, the introduction of the pentamethylcyclopentadienyl ligand into the tetranuclear cluster influences the ligand geometry and mobility, and could lead to differing substitution products to those obtained from the normal cyclopentadienyl system.

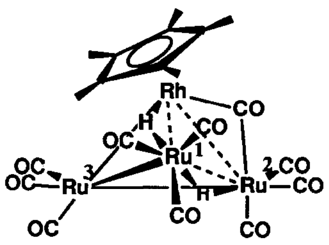

4a
(solid state structure)

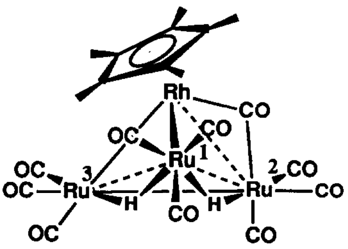

4b

The reaction of **4** with triphenylphosphine at ambient temperature afforded only two simple substituted clusters, $[RhRu_3(\mu\text{-}H)_2(\mu\text{-}CO)(CO)_{9-n}(PPh_3)_nCp^\star]$ ($n = 1$, **7**; $n = 2$, **8**), of analogous stoichiometry to the products obtained from the related reaction of **1**. Other cleavage products of this reaction included the simple derivatives $[Ru_3(CO)_{12-n}(PPh_3)_n]$ ($n = 1$ and 3) [10], not observed in the reaction of **1**, and some uncharacterised compounds containing $RhCp^\star$.

Cluster **7** was obtained as dark brown prisms after crystallisation from petroleum ether. The ^1H NMR spectrum in CD_2Cl_2 at 25 °C is consistent with a single, geometrically rigid system and the two doublet metal hydride resonances (see Table 1) have chemical shifts comparable to those of the isomer **4b** of the parent cluster **4**. The doublet couplings were assigned to $^{31}P\text{–}^1H$ interactions on the basis of ^{31}P decoupling experiments and the values of the constants are consistent with the presence of a *cis*-$^{31}P\text{–Ru–H}$ unit (9.9 Hz) and of a longer range, possibly three-bond, $^{31}P\text{–H}$ interaction (2.8 Hz). The absence of a significant coupling to ^{103}Rh rules out a structure containing a hydrogen directly bonded to the rhodium atom. The ^1H NMR spectrum is essentially unchanged at temperatures down to −90 °C, although at −50 °C slightly better resolution revealed a very small, secondary doublet coupling (ca. 0.7 Hz) in the higher frequency hydride resonance (−13.07 ppm) and this may arise from either a weak Rh–H or H–H interaction. The $^{31}P\{^1H\}$ NMR spectrum comprises a singlet (half-width 7 Hz) with no detectable coupling to Rh, and the IR spectrum contains only one prominent $\nu(\mu\text{-CO})$ band at 1822 cm^{-1}.

On the basis of the above spectroscopic data structure **7a** or **7b** can be considered for cluster **7**. Isomer **7b** is analogous to the structure assigned to the minor isomer of

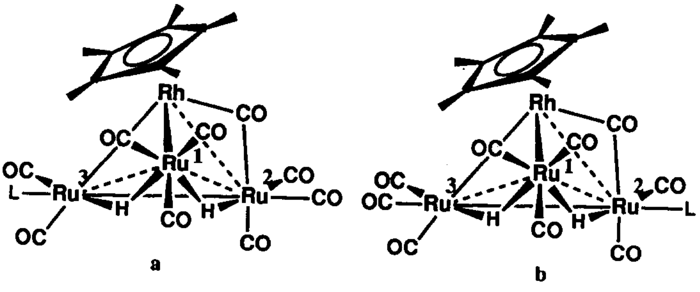

a

b

7 L = PPh_3

2, i.e. **2b**, and includes a phosphine ligand coordinated equatorially to Ru(2), as found for one phosphine in crystalline **3**. Structure **7a** is analogous to the undetected isomer **2c** of cluster **2**. Both **7a** and **7b** are consistent with the ^1H NMR analysis but, by comparison with the phosphine derivatives containing a normal cyclopentadienyl ligand, cluster **7b** might be expected to exhibit a *J*(Rh–P) coupling constant in the $^{31}P\{^1H\}$ NMR spectrum of ca. 20 Hz, and also display a lower frequency $\nu(\mu\text{-CO})$ vibration in the IR spectrum. Therefore **7a** seems the more likely structure, although alternative axial coordination of the PPh_3 ligand at either Ru(3) or Ru(2) cannot be ruled out. It should be noted that ^1H NMR spectra of some non-recrystallised samples of this product did show additional, small hydride resonances around −17 ppm which may originate from alternative isomers.

Cluster **8** was obtained as a crystalline solid, solvated with dichloromethane. In solution at 25 ° C well-resolved ^1H NMR resonances, typical of a geometrically rigid system, were observed (see Table 1). Following the discussion above for cluster **7** and by comparison with the data for cluster **3**, the ^1H and $^{31}P\{^1H\}$ NMR spectra of the dominant form can be assigned a geometry **8a** or **8b**. However, the small *J*(Rh–H) coupling constant of the ^{31}P resonance at 41.6 ppm (3.1 Hz) and undetectable Rh–H coupling to the resonance at 29.9 ppm (half-width 6 Hz) would lend support to structure **8b**. The IR spectrum includes three weak, or very weak, bands in the region of bridging-CO vibrations and it seems likely that more than one isomer is present in solution; also, low intensity resonances observed in the ^1H NMR spectrum may arise from an alternative form (see Experimental Section).

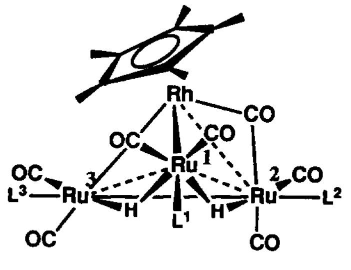

8a $L^1 = L^2 = PPh_3$, $L^3 = CO$
8b $L^1 = L^3 = PPh_3$, $L^2 = CO$

It is interesting that the principal phosphine substitution products of the pentamethylcyclopentadienyl cluster **4** have structures with two bridging hydrogen atoms around the Ru_3 basal plane, as found for the normal cyclopentadienyl derivatives, and not as found in the main form of the parent cluster. However, contrary to the cyclopentadienyl system, the most stable isomer of the mono-phosphine cluster **7** does not involve phosphorus coordination at Ru(1) and a more geometrically rigid isomer is produced.

Experimental

All reactions were carried out using Schlenk techniques under an atmosphere of dry, gaseous nitrogen using freshly distilled, predried solvents, as previously described [5]. Starting clusters $[RhRu_3(\mu\text{-}H)_2(\mu\text{-}CO)(CO)_9Cp]$ (**1**) and $[RhRu_3(\mu\text{-}H)_2(\mu\text{-}CO)(CO)_9Cp^\star]$ (**4**) were prepared as reported [3]. Ligands PPh_3 (BDH) and $P(OMe)_3$ (Aldrich) were obtained commercially and used as supplied. Silica gel used for column chromatography was 70–230 mesh (Merck) and petroleum ether had a boiling range 60–80 °C, unless otherwise specified. NMR spectra were recorded on a Bruker WP 200 SY spectrometer at 200 MHz for ^1H, using $SiMe_4$ as reference, and at 81.0 MHz for ^{31}P, with 85% H_3PO_4 as reference, at ca. 25 °C, unless otherwise stated. IR spectra were obtained on a Perkin Elmer 580 spectrometer and FAB mass spectra on a Kratos MS 50 TC instrument from matrices in *m*-nitrobenzylalcohol at the University of Edinburgh. Elemental analyses were determined at UMIST, Manchester and/or at the University of Edinburgh.

Reaction of cluster 1 with triphenylphosphine

This reaction was carried out in THF as previously reported [5]. After chromatography with petroleum ether/dichloromethane in 5/1 and 1/1 mixtures, respectively, $[RhRu_3(\mu\text{-}H)_2(\mu\text{-}CO)(CO)_8(PPh_3)Cp]$ (**2**) and $[RhRu_3(\mu\text{-}H)_2(\mu\text{-}CO)(CO)_7(PPh_3)_2Cp]$ (**3**), were obtained and identified from reported spectroscopic data [5]. Continued chromatography with dichloromethane/acetone eluted at least two different bands: the major product was an orange solid; IR (CH_2Cl_2) ν(CO): 2060 s, 2025 vs, 1998 s, 1958 s, cm^{-1}; ^1H NMR ($CDCl_3$) 7.4 ppm (br, mult.).

Reaction of cluster 1 with trimethylphosphite

Cluster **1** (80 mg, 0.106 mmol) and $P(OMe)_3$ (0.11 mmol) in THF (10 cm^{-1}) were stirred for 5 h at room temperature. The solution was evaporated to dryness in the presence of a little silica gel and the resulting solid residue was chromatographed on a column of silica gel. Petroleum ether eluted $[Rh(CO)_2Cp]$ and petroleum ether/dichloromethane, 10/1, gave some unreacted **1**.

Petroleum ether/dichloromethane, 3/1, eluted an orange-brown band which gave an oily brown product after evaporation of solvent (ca. 5 mg). Recrystallisation from petroleum ether gave brown crystals (still somewhat oily) of slightly impure $[RhRu_3(\mu\text{-}H)_2(\mu\text{-}CO(CO)_8\{P(OMe)_3\}Cp]$ (**5**). IR (petroleum ether) ν(CO): 2070 m, 2049 sh, 2040 vs, 2005 m, 1991 m, 1823 m, 1789 vw, cm^{-1}; ^1H NMR (CD_2Cl_2) 5.74 (s, 5H, C_5H_5), 3.62 (d, J(P–H) = 12 Hz, 9H, CH_3), −17.13 (d, (br), J(P–H) = 8.6 Hz, 2H, Ru–H) ppm; FAB-MS: M^+ and $(M-n\text{CO})^+$, $n = 1$–9, {but also small ion peaks at $(M+m\text{CO})^+$, $m = 1$–3}.

Dichloromethane eluted a yellow band which on evaporation of solvent and recrystallisation from petroleum ether/dichloromethane, yielded brown crystals (ca. 3 mg) of $[RhRu_3(\mu\text{-H})_2(\mu\text{-CO})(CO)_7\{P(OMe)_3\}_2Cp]$ (**6**). Anal. Found C, 24.4; H, 2.7; $C_{19}H_{25}O_{14}P_2RhRu_3$ calc. C, 24.1; H, 2.7%. IR (petroleum ether) ν(CO): 2048 s, 2025 s, 2000 sh, 1985 vs, 1782 m, cm^{-1}; ^1H NMR ($CDCl_3$) 5.70 (s, 5H, C_5H_5), 3.62 (d, J(P–H) = 12.3 Hz, 18H, CH_3), −16.3 (br, 1H, Ru–H), −17.9 (br, 1H, Ru–H) ppm, {at −25 ° C, the latter two resonances become resolved and were assigned by selective decoupling: −16.25 (ddd, $J(P^1\text{–}H)$ = 10.4, $J(P^2\text{–}H)$ = ca. 2.4, J(H–H) = ca. 2.4 Hz) and −18.05 (ddd, $J(P^1\text{–}H)$ = ca. 9, $J(P^2\text{–}H)$ = ca. 9, J(H–H) = ca. 2.4 Hz)} ppm.

Acetone/dichloromethane and acetone alone eluted small brown bands of unidentified carbonyl containing products, leaving some material on the column.

*Reaction of cluster **4** with triphenylphosphine*

Cluster **4** (50 mg, 0.061 mmol) and PPh_3 (18 mg, 0.069 mmol) in THF (15 cm^3) were stirred at ambient temperature for 24 h. The solution was evaporated to dryness and chromatographed as above on silica gel. Petroleum ether/dichloromethane, 10/1, eluted a little unreacted **4**.

Petroleum ether/dichloromethane, 4/1, eluted an orange band which yielded $[RhRu_3(\mu\text{-H})_2(\mu\text{-CO})(CO)_8(PPh_3)Cp^*]$ (**7**) on evaporation (ca. 10 mg), obtained as brown crystals on recrystallisation from petroleum ether at −15 ° C. Anal. Found C, 42.3; H, 3.8; $C_{37}H_{32}O_9PRhRu_3$ calc. C, 42.0; H, 3.1%. IR (Petroleum ether) ν(CO): 2061 s, 2036 vs, 2021 m, 1998 s, 1985 ms(br), 1822 m, cm^{-1}. ^1H NMR (CD_2Cl_2) 7.5 (mult., 15H, C_6H_5), 1.73 (d, J(Rh–H) = 0.7 Hz, 15H, $C_5(CH_3)_5$), −13.01 (d, J(P–H) = 9.9 Hz, 1H, Ru–H), −20.62 (d, J(P–H) = 2.8 Hz, 1H, Ru–H) ppm.

Petroleum ether/dichloromethane, 2/1, eluted a yellow band giving, on evaporation of the solvent, an oily product which after recrystallisation from the same mixed solvent gave $[RhRu_3(\mu\text{-H})_2(\mu\text{-CO})(CO)_7(PPh_3)_2Cp^*]$ (**8**) as small dark brown prismatic crystals solvated with CH_2Cl_2 (ca. 6 mg). Anal. Found C, 48.0; H, 3.9; $C_{54}H_{47}O_8P_2RhRu_3 \cdot CH_2Cl_2$ calc. C, 48.0; H, 3.6%. IR (petroleum ether) ν(CO): 2048 vs, 2037 sh, 2010 m, 1985 s, 1968 sh, 1958 ms, 1819 w(sh), 1800 w, 1756 vw, cm^{-1}. ^1H NMR ($CDCl_3$) 7.7–7.2 (complex mult., 30H, C_6H_5), 5.28 (s, ca. 2H, CH_2Cl_2), 1.77 (s, 15H, $C_5(CH_3)_5$), −12.28 (ddd, J(P–H) = 13.2 and 7.8 Hz, $J < 1$ Hz, ca. 1H, Ru–H), −20.34 (dd, J(P–H) = 10.2 and 2.8 Hz, ca. 1H, Ru–H) ppm {NB: a small amount (< 15%) of isomer (or impurity) displayed resonances assignable to Ru–H atoms at −14.10 (s, 1H) and −20.78 (d, ca. 1 Hz, 1H) ppm}.

Petroleum ether/dichloromethane, 1/1, eluted a red band which gave an amorphous red solid on evaporation (ca. 5 mg). This was shown by IR and NMR spectroscopy to be mixture of compounds $[Ru_3(CO)_{12-n}(PPh_3)_n]$ (n = 1–3). Rechromatography of this mixture separated pure $[Ru_3(CO)_{11}(PPh_3)]$ (Anal. Found C, 39.9; H, 3.1; $C_{29}H_{15}O_{11}PRu_3$ calc. C, 39.9; H, 1.7%); and deep maroon crystals of $[Ru_3(CO)_9(PPh_3)_3]$: IR (petroleum ether) ν(CO): 2050 vw, 1987 sh, 1978 s, cm^{-1} (cf. literature [10] (benzene): 2044 vw, 1978 sh, 1967 s); ^1H NMR ($CDCl_3$) 7.4 ppm (mult., C_6H_5).

Dichloromethane/acetone, 1/1, eluted a red/brown band which yielded a mixture of solid products (ca. 4 mg): uncharacterised carbonyl compounds containing Cp^*Rh and PPh_3 units. Finally, methanol eluted a very small amount of yellow material, leaving a dark band on the column.

Crystal structure determination of $[RhRu_3(\mu\text{-}H)_2(\mu\text{-}CO)(CO)_7(PPh_3)_2Cp]$ *(3)*

A single crystal of **3** (from dichloromethane–hexane at −15 °C, approximate size 0.6 × 0.2 × 0.08 mm), mounted in a Lindemann tube, was used for X-ray data collection.

Crystal data. $C_{49}H_{37}O_8P_2RhRu_3$, $M = 1221.85$, dark red-brown plates, triclinic, space group $P1$ (No. 2), a 10.5144 (17), b 11.541 (3), c 19.736 (4) Å, α 90.868 (21), β 85.890 (18), γ 105.216 (19)°, U 2304.9 Å^3, $Z = 2$, D_c 1.760 g cm^{-3}, $F(000)$ 1204, μ(Mo-K_α) 66.19 cm^{-1}.

Data collection. The intensity data were collected on an Enraf–Nonius CAD4 diffractometer over the hemisphere (h: 0–12, k: -13–$+13$, l: -23–$+23$) using graphite-monochromated Mo-K_α X-radiation (λ 0.710693 Å) and ω–2θ scanning. Of the 8096 unique data measured, 6117 and $I > 2\sigma(I)$ and were used in subsequent structural solution and refinement. The data were corrected for Lorentz and polarisation effects, and for absorption (DIFABS [11]).

Structure solution. The approximate locations of the Rh, Ru and P atoms were determined by direct methods (SHELXS86 [11]). After two cycles of refinement, the remaining non-hydrogen atoms were subsequently located from a difference Fourier map phased on the refined heavy atom positions. The structure was refined by full-matrix least squares methods (SHELX76 [11]) using anisotropic temperature factors for all the non-hydrogen atoms, except the disordered carbon atoms of the cyclopentadienyl ring (two-site disorder, relative populations 79 : 21). All the hydrogen atoms were located on difference Fourier maps and included in the refinement process at idealised positions except for the bridging hydrogen atoms H(1) and H(2) whose positional and isotropic thermal parameters were allowed to refine as normal. The phenyl and cyclopentadienyl rings were treated as idealised hexagons (C–C 1.395 Å, C–H 0.95 Å) and pentagons (C–C 1.420 Å, C–H 0.95 Å), respectively, with fixed anisotropic temperature factors for the hydrogen atoms (U_{iso} 0.10 Å^2). At convergence, the discrepancy factors R and R_w were 0:029 and 0.039, respectively. The weighting scheme, $w^{-1} = [\sigma^2(F) + 0.000584(F)^2]$ was found to give satisfactory analyses of variance. The final difference Fourier map was essentially featureless, general noise level less that ±0.32 e Å^{-3}, from four peaks ca. 0.87–0.77 e Å^{-3} of no apparent chemical significance in the region around the metal cluster. Incidental crystallographic calculations and compilation of tables were carried using the computer program CALC [11]. Lists of refined thermal parameters and calculated and observed structure factors are available on request from the authors.

Acknowledgements

We thank Professor M.B. Hursthouse for collection of X-ray data through the SERC X-ray data service, Mr. A.T. Taylor, University of Edinburgh, for recording FAB mass spectra, and Johnson Matthey Technology Centre for the loan of ruthenium and rhodium compounds.

References

1 E.G. see: (a) D.A. Roberts and G.L. Geoffroy, in G. Wilkinson, F.G.A. Stone and E.W. Abel (Eds.), Comprehensive Organometallic Chemistry, Pergamon Press, Oxford, 1982, Ch. 40; (b) R.D. Adams, Polyhedron, 7 (1988) 2251 (and following papers of this "Symposium in Print").

2 E.G. see: P. Braunstein and J. Rose, in I. Bernal (Ed.), Stereochemistry of Organometallic and Inorganic Compounds, Vol. 3, Elsevier, Amsterdam, 1989, p. 1.

3 W.E. Lindsell, C.B. Knobler and H.D. Kaesz, J. Organomet. Chem., 296 (1985) 209.

4 W.E. Lindsell and K.J. McCullough, J. Organomet. Chem., 346 (1988) 425.

5 W.E. Lindsell, N.M. Walker and A.S.F. Boyd, J. Chem. Soc., Dalton Trans., (1988) 675.

6 J.R. Fox, W.L. Gladfelter, T.G. Wood, J.A. Smegal, T.K. Foreman, G.L. Geoffroy, I. Tavanaiepour, V.W. Day and C.S. Day, Inorg. Chem., 20 (1981) 3214; W.L. Gladfelter, J.R. Fox, J.A. Smegal, T.G. Wood and G.L. Geoffroy, Inorg. Chem., 20 (1981) 3223; see also: G.L. Geoffroy, Acc. Chem. Res., 13 (1980) 469.

7 E. Sappa, M.L.N. Marchino, G. Predieri, A. Tiripicchio and M.T. Camellini, J. Organomet. Chem., 307 (1986) 97.

8 B.T. Huie, C.B. Knobler and H.D. Kaesz, J. Am. Chem. Soc., 100 (1978) 3059.

9 D. Labroue, R. Queau and R. Poilblanc, J. Organomet. Chem., 186 (1980) 101.

10 M.I. Bruce, G. Shaw and F.G.A. Stone, J. Chem. Soc., Dalton Trans., (1972) 2094; M.I. Bruce, J.G. Matisons and B.K. Nicholson, J. Organomet. Chem., 247 (1983) 321.

11 G.M. Sheldrick, SHELXS86, University of Göttingen, Germany, 1986; SHELX76, University of Cambridge, England, 1976; N.G. Walker and D. Stuart DIFABS, Acta Crystallogr., A39 (1983) 158; R.O Gould and P.J. Taylor, CALC, University of Edinburgh, Scotland, 1983; C.K. Johnson, ORTEP, Report ORNL-5183, Oak Ridge National Laboratory, Tennessee, 1976; W.D.S. Motherwell, PLUTO, University of Cambridge, England, 1976.